AN EXPERIMENTAL COMPARISON BETWEEN THE CONTINUUM AND SINGLE JUMP DESCRIPTIONS OF NONACTIN-MEDIATED POTASSIUM TRANSPORT THROUGH BLACK LIPID MEMBRANES

CEES VAN DIJK AND ROBERT DE LEVIE
Department of Chemistry, Georgetown University, Washington, D.C. 20057

ABSTRACT The continuum and single jump treatments of ion transport through black lipid membranes predict experimentally distinguishable results, even when the same mechanistic assumptions are made and the same potential-distance profile is used. On the basis of steady-state current-voltage curves for nonactin-mediated transport of potassium ions, we find that the continuum model describes the data accurately, whereas the single jump model fails to do so, for all cases investigated in which capacitance measurements indicate that the membrane thickness varies little with applied potential.

INTRODUCTION

Artificial planar black lipid membranes have been used widely as models for biological plasma membranes. Mueller et al. (1962*a*, 1962*b*, 1963) developed a method to make such ultrathin membranes from dilute solutions of lipids in organic solvents. Unfortunately, depending on the solvent used, some of it may remain in these membranes (Andrews et al., 1971; Fettiplace et al., 1971; Pagano et al., 1972; Bunce and Hider, 1974) and may affect their properties.

The incorporation of solvent was reduced considerably by Montal and Mueller (1972; see also Montal, 1973; Benz et al., 1975) when they used an alternative method, first described by Takagi et al. (1965), based on the fusion of two monolayers. Artificial planar membranes made by either technique have played a major role in establishing the qualitative and quantitative description of ion transport through biological membranes, and are still doing so.

There are two main approaches to the quantitative description of ion transport through black lipid membranes. In the first one considers the membrane interior as a hydrocarbonlike continuum of low dielectric permittivity. Such a macroscopic region, interposed between two aqueous solutions, forms an effective barrier to ion transport, given the Born energy (Born, 1920; Finkelstein and Cass, 1968; Parsegian, 1969; Neumcke and Läuger, 1969) required to bring an ion from a region of high to one of low permittivity. Transport through such a hydrocarbonlike liquid phase can be described in terms of the classical Nernst-Planck equations (Nernst, 1888, 1889; Planck, 1890). Because of the Born energy, the solubility of ions in the membrane interior will usually be quite low, in which case the Nernst-Planck equations can be simplified considerably, and lead to the constant field approximation (Mott, 1937; Goldman, 1943; MacGillivray and Hare, 1969; de Levie and Moreira, 1972; de Levie et al., 1972).

The second approach is based on the fact that the entire thickness of the hydrocarbon region of black lipid membranes is often of the order of only 2 to 3 nm, too thin to be considered a macroscopic phase. An ion permeating such a membrane is always close enough to an interface to sense the proximity of the aqueous phases, through both dipole potentials and image forces. This led to considering the entire membrane as a single activation energy barrier (Markin, 1969; Läuger and Stark, 1970; Ketterer et al., 1971). The resulting single jump model, which describes ion transport in terms of chemical rate equations, also leads to a very simple mathematical formalism.

The macroscopic description of ion transport given by the constant field approximation might be expected to apply to a hydrocarbon layer with a thickness of, say, 30 nm, such that interfacial effects are relatively unimportant. Likewise, the single jump model might be expected to apply to distances of the order of the diameter of a —CH_2-group, i.e., of perhaps 0.3 nm. Unfortunately, though not by accident (de Levie, 1978), the actual width of the hydrocarbon region in black lipid membranes is intermediate between these values, and neither simple model can be expected to yield a reliable description. Therefore, efforts have been made to modify the above approaches.

For the continuum approach, one can introduce interfa-

Dr. van Dijk's permanent address is the Institute of Applied Chemistry, T.N.O., Postbus 108, 3700 AC Zeist, the Netherlands.

cial effects by rounding the potential-distance profile near the membrane-water interfaces in an effort to represent the effects of dipole and image forces. Such rounding can be achieved with either a continuous algebraic function (Hall et al., 1973; de Levie, 1978) or by using a trapezoidal profile (Hall et al., 1973; Hladky, 1974). The latter approach is selected here since it facilitates direct comparison with the single jump formalism.

Hall et al. (1973) modified the single jump formalism so that it could account for rectification (observed, e.g., with dissimilar concentrations of membrane-permeable ions on either side of the membrane) without having to consider finite rates of interfacial reactions (Stark, 1973). To this end they considered the single jump model for a trapezoidal potential-distance profile. It seems germane to investigate whether these two approaches, each generalized by using the same trapezoidal profile, will become indistinguishable or, if not, which one better describes experimental observations.

In the context of the single jump model, the use of a potential-distance profile needs some justification, because the single jump treatment does not require a profile, but only a barrier height. Nonetheless a profile is convenient as a conceptual aid in visualizing how the barrier height varies with applied voltage. For example, the original single jump model can be considered to be based on the profile of an isosceles triangle superposed on a constant-field baseline, the latter accounting for the effect of the external potential. It is in this limited sense, of a conceptual aid in specifying the barrier height and its dependence on applied voltage, that we use a profile in the single jump formalism.

We emphasize that the trapezoidal profile used here in conjunction with both model approaches contains an adjustable parameter, with a numerical value which is to be determined experimentally. The continuum model regains its original form when the present continuum approach is used in conjunction with $\beta = 0$, which expands the trapezoid into a rectangle. Likewise, the original single jump formalism is recovered from our single jump treatment when used with $\beta = 0.5$, in which case the trapezoid is collapsed into a triangle. Thus, the trapezoidal profile assumed here extends the original continuum and single jump models in such a way as to include their original forms. A comparison between these treatments, using the same assumed profile, allows us to focus on the validity of the basic assumptions involved in these models.

Such a comparison is useful because it turns out that, even when they are based on the same mechanistic assumptions, and on the same potential-distance profile, the predictions of the continuum and single jump models are not identical, because these same assumptions are used in different ways in the two approaches. In the continuum formalism, the concentrations of ions and molecules in the membrane are treated as continuous functions of distance across the membrane, and the entire potential-distance profile is used, together with the macroscopic laws of electrodiffusion, to describe transport. In the single jump approach all molecules and ions in the membrane are taken as concentrated on the two sides of the barrier, of which only the maximum height is used, the detailed barrier shape being of no consequence whatever.

THEORY

In this section we will consider two different ion permeation mechanisms, namely, those of lipid-soluble cations and of cation transport mediated by a neutral carrier, even though the experiments reported here involve only the latter. The results derived here should be applicable to anions as well, after incorporation of their negative valency in the equations. However, lipid-soluble anions typically exhibit strong adsorption, which complicates the description of their permeation behavior. Moreover, these anions move so readily through a black lipid membrane that their membrane permeation rate is, often, limited by aqueous diffusion.

As our test system we use nonactin-mediated potassium transport that, under our experimental conditions, behaves as limited only by the membrane permeation of the potassium-nonactin complex. Below, then, we will consider for both the continuum and single jump models the steady-state current-voltage expressions for lipophilic cations and for cation transport mediated by a neutral carrier.

In both models, the potential-distance profile across the membrane will be taken to be the sum of an intrinsic profile and a perturbation due to the externally applied potential. (The concentration of ions in the membrane is assumed to be so low that its effect on the profile can be neglected.) The intrinsic profile stems mostly from differences in solvation energy between molecules in the membrane interior and those in the surrounding aqueous solutions. For ions, it also includes the combined effects of the Born energy, of image forces, and of dipole potentials. The influence of the applied potential will, in both cases, be described in terms of a constant field approximation, i.e., the additional, external potential will be taken to be a linear function of distance across the membrane.

To keep the mathematics as simple as possible, we will make several simplifying assumptions, all of which are believed to be applicable to the system considered here under the experimental conditions used. Aqueous transport will not be taken into account, i.e., the aqueous cation concentrations will be treated as uniform throughout the aqueous phases. Furthermore, we will assume that the rates of phase transfer, i.e., those of both entering and leaving the membrane for lipophilic cations, or those of the formation and dissociation of the cation-carrier complex, are sufficiently fast so as not to be rate limiting. (This restrictive assumption will be relaxed in Appendix A.) Moreover, nonactin will be assumed to be confined to the membrane, and its concentration there will be taken to be in large excess over that of its potassium complex in the membrane. Surface charges will not be taken into account, and the lipid composition will be assumed to be the same on both sides of the membrane, so that the potential-distance profile in the absence of an applied potential can be taken to be symmetrical with respect to a plane through the middle of the membrane. Last but not least, the membrane thickness d will be assumed to be independent of time or applied potential. All of these assumptions will, of course, be made for both models.

The Continuum Model

The continuum description of ion transport starts from the Nernst-Planck equation (Nernst, 1888, 1889; Planck, 1890), which, for a monovalent cation, reads

$$\frac{\partial c_M}{\partial t} = D_M \frac{\partial}{\partial x}\left(\frac{\partial c_M}{\partial x} + c_M \frac{\partial \psi}{\partial x}\right), \quad (1)$$

where c_M denotes the volume concentration of the ion in the membrane, and D_M its diffusion coefficient, which is assumed to be independent of the

distance x across the membrane. The (intrinsic plus external) potential (in units of kT/e in order to make it dimensionless) is denoted by ψ. In the steady state, $\partial c_M/\partial t = 0$, and Eq. 1 can be integrated to

$$-\frac{I}{FD_M} = \frac{dc_M}{dx} + c_M \frac{d\psi}{dx}, \tag{2}$$

where $-I/FD_M$ is the integration constant, and hence must be independent of distance x. Eq. 2 can be recast as

$$-\frac{I}{FD_M} e^{\psi} = \frac{d}{dx}(c_M e^{\psi}), \tag{3}$$

which can be integrated once more, from one side of the membrane to the other, to yield

$$\frac{I}{FD_M}\int_0^d e^{\psi}\,dx = c_{M0} - c_{M1}e^{-\upsilon} \tag{4}$$

where d is the membrane thickness, and the indices 0 and 1 denote values at $x/d = 0$ and $x/d = 1$, respectively.

The integral in Eq. 4 can be evaluated for the trapezoidal profile of Fig. 1 as

$$\begin{aligned}\int_0^d e^{\psi}dx &= \int_0^{\beta d} e^{x(\psi_0-\beta\upsilon)/\beta d}\,dx \\ &+ \int_{\beta d}^{(1-\beta)d} e^{\psi_0 - x\upsilon/d}\,dx + \int_{(1-\beta)d}^{d} e^{\psi_0/\beta - x(\psi_0+\beta\upsilon)/\beta d}\,dx \\ &= \left(\frac{e^{-\beta\upsilon}}{\psi_0-\beta\upsilon} - \frac{e^{(\beta-1)\upsilon}}{\psi_0+\beta\upsilon}\right)\frac{\psi_0 d}{\upsilon}e^{\psi_0} - \left(\frac{\beta d}{\psi_0-\beta d} + \frac{\beta d e^{-\upsilon}}{\psi_0+\beta d}\right).\end{aligned} \tag{5}$$

Because $\psi_0 \gg \upsilon$, the terms in Eq. 5 which are multiplied by e^{ψ_0} dominate, and we can therefore use the approximation

$$\int_0^d e^{\psi}\,dx \approx e^{\psi_0}\,[e^{-\beta\upsilon} - e^{(\beta-1)\upsilon}]\,d/\upsilon. \tag{6}$$

This result is the same as would have obtained by evaluating only for the central portion of the profile, for x values between βd and $(1-\beta)d$. Thus, the effect of using a trapezoidal barrier is, for all practical purposes, identical to that of using a rectangular intrinsic barrier of reduced width $(1-2\beta)d$.

For a lipophilic cation, assuming equilibrium between the cation concentrations at both sides of the interface, i.e.,

$$c_{M0} = Kc_{W0}, \qquad c_{M1} = Kc_{W1} \tag{7}$$

where c_W denotes an aqueous concentration and K a partition coefficient, Eqs. 4, 6, and 7 yield the current-voltage relation

$$I = \frac{FD_M K\upsilon\,(c_{W0} - c_{W1}\,e^{-\upsilon})}{e^{\psi_0}\,d\,[e^{-\beta\upsilon} - e^{(\beta-1)\upsilon}]}. \tag{8}$$

For carrier-mediated cation transport, with the neutral carrier in large excess over the cation-carrier complex, we have instead

$$c_{M0} = K_N c_N c_{W0}, \qquad c_{M1} = K_N c_N c_{W1} \tag{9}$$

where c_N is the concentration of the neutral carrier in the membrane (taken to be independent of x because of its assumed excess with respect to c_M), and K_N the equilibrium constant for the formation and dissociation of the cation-carrier complex. In this case, the current-voltage curve follows from Eqs. 4, 6, and 9 as (Hladky, 1974; Schoch et al., 1979)

$$I = \frac{FD_M K_N c_N \upsilon\,(c_{W0} - c_{W1}e^{-\upsilon})}{e^{\psi_0} d[e^{-\beta\upsilon} - e^{(\beta-1)\upsilon}]}. \tag{10}$$

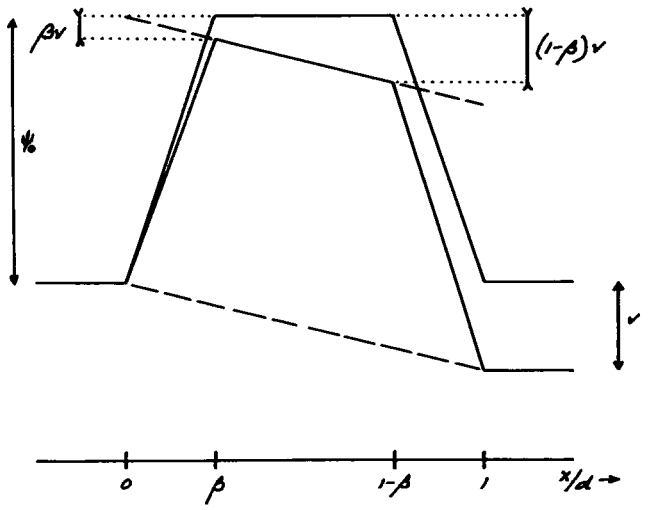

FIGURE 1 The trapezoidal potential-distance profile used in the absence (*top* curve) or presence (*bottom* curve) of an externally applied voltage. Potentials ψ and υ are made dimensionless by expressing them in units of kT/e and, likewise, distance x across the membrane is divided by membrane thickness d.

The Single Jump Model

In the single jump approach, ion transport across the membrane is described as that across a single activation energy barrier. The intrinsic barrier is considered to be so high that the externally applied potential constitutes only a minor perturbation on the total barrier shape and, specifically, can be taken not to affect the position of the maximum in the resulting overall potential-distance profile.

Because of the assumed height of the barrier, only a negligible fraction of the ions and molecules in the membrane will, at any time, reside in the region of the barrier maximum. Therefore, all ions and molecules are assumed to be located in the positions of energy wells on both sides of the barrier. The formalism reflects this by expressing their concentrations in terms of the number of moles per unit membrane area, i.e., as surface rather than volume concentrations.

For a lipophilic cation, the current can be written as

$$I = F\,(\vec{k}n_{M0} - \overleftarrow{k}n_{M1}) \tag{11}$$

where I is the current density, F the Faraday, $\vec{k}$ and $\overleftarrow{k}$ are the potential-dependent rate constants for ion transport from side 0 to side 1 of the membrane and vice versa, and n_{M0} and n_{M1} are the surface concentrations of the cation in the membrane at sides 0 and 1, respectively.

The above equations must be combined with specific expressions for the potential-dependence of the rate constants $\vec{k}$ and $\overleftarrow{k}$. For the trapezoidal intrinsic profile of Fig. 1 *a*, application of a potential υ (in units of kT/e in order to make it dimensionless) lowers the barrier height for ion transport from side 0 to side 1 by υ, while raising it in the reverse direction by $(1-\beta)\upsilon$, so that

$$\vec{k} = k^{\circ}e^{\beta\upsilon}, \qquad \overleftarrow{k} = k^{\circ}e^{(\beta-1)\upsilon}, \tag{12}$$

where k° represents the rate constant for the ion-carrier complex crossing the intrinsic barrier, i.e., for $\upsilon = 0$. Combination of Eqs. 11 and 12 yields

$$I = FKk^{\circ}e^{\beta\upsilon}\,(c_{W0} - c_{W1}e^{-\upsilon}) \tag{13}$$

where $K = c_{W0}/n_{M0} = c_{W1}/n_{M1}$ has the function, though not quite the dimension, of a partition coefficient. For nonactin-mediated potassium transport, again assuming that the neutral carrier is present in the

membrane in large excess so that $n_{N0} \gg n_{M0}$, $n_{N1} \gg n_{M1}$ and $n_{N0} - n_{N1} = n_N$, we find instead

$$I = FK_N n_N k^o e^{\beta v} (c_{W0} - c_{W1} e^{-v}). \quad (14)$$

Comparison of the Two Models

We note that, for the continuum as well as for the single jump model, a conductance function $S(v)$ can be defined (Hall et al., 1973), which is independent of the aqueous concentrations c_{W0} and c_{W1}

$$S(v) = \frac{c_{W0} e^{v/2} - c_{W1} e^{-v/2}}{I} = \frac{c_{W0} - c_{W1} e^{-v}}{I e^{-v/2}}. \quad (15)$$

For the continuum model we find, from Eqs. 8 and 10, after normalization (de Levie and Abbey, 1976) through division by $S(v = 0)$

$$s = \frac{S(v)}{S(v = 0)} = \frac{\sinh (1/2 - \beta)v}{(1/2 - \beta)v} \quad (16)$$

while the single jump results of Eqs. 13 and 14 lead to

$$s = e^{(1/2-\beta)v}. \quad (17)$$

When β does not have a value close to 1/2, Eqs. 16 and 17 predict quite different dependencies of the functions S and s on the applied voltage v,

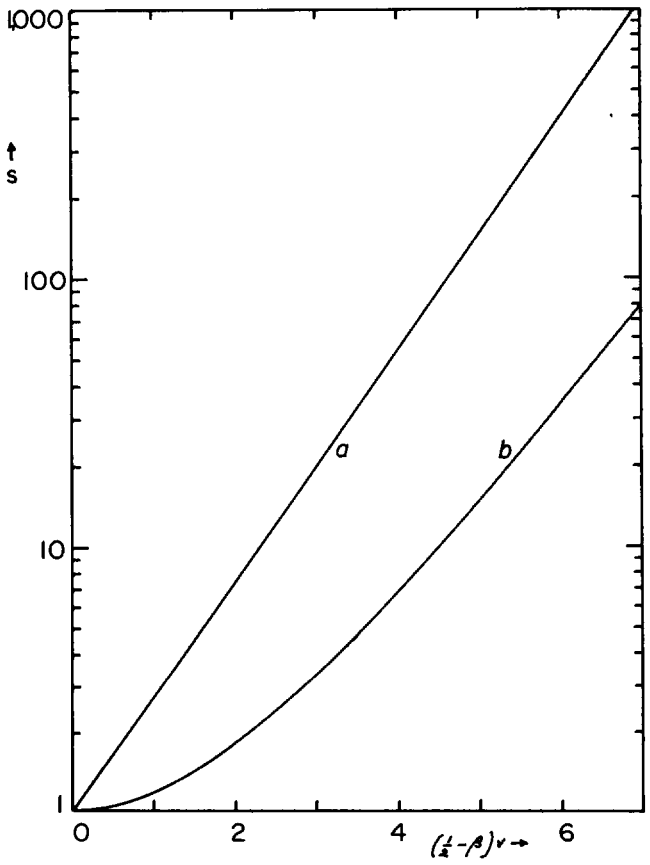

FIGURE 2 Semilogarithmic plot of the dimensionless conductance function s vs. $(1/2 - \beta)v$, where v is the dimensionless potential for ion transport in *a*, the single jump model (Eq. 17), and *b*, the continuum model (Eq. 16).

even for the same mechanistic assumptions and for the same assumed potential-distance profile $\psi(x)$.

Fig. 2 illustrates the different predicted behaviors, and shows that a semilogarithmic plot of S or s vs. v will be linear for the single jump model, but curved when the continuum model applies. Consequently, it may be possible to distinguish, experimentally, which model best describes the observed behavior. We emphasize again that this criterion will fail when $\beta \approx 1/2$.

MATERIALS AND METHODS

All salts used (KCl, LiCl, $CaCl_2$) were Baker "analyzed;" *n*-hexane was also from J. T. Baker Chemical Co. (Phillipsburg, NJ), while *n*-decane and *n*-octadecane were from Eastman-Kodak Co., (Rochester, NY) and squalene from Sigma Chemical Co., (St. Louis, MO). Throughout this study we used synthethic L-diphytanoyllecithin from Avanti Polar Lipids, Inc., (Birmingham, AL). Nonactin was from Boehringer Mannheim Diagnostics Inc. (Houston, TX). All chemicals were used without further purification.

Currents were measured with laboratory-assembled polarographic equipment based on operational amplifiers. An initial voltage, a slowly changing voltage from an integrator, and an alternating voltage from an oscillator (Krohn-Hite 4002; Krohn-Hite Corp., Avon, MA) were mixed in a potentiostat and applied to the cell containing the membrane. The resulting membrane current was converted into a voltage by a carefully shielded, battery-operated operational amplifier (Analog Devices AD 515 LH; Analog Devices, Inc., Norwood, MA) using feedback resistances from 10^6 to 10^{11} Ω. Two XY-recorders (Hewlett-Packard 7005B; Hewlwett-Packard Co., Palo Alto, CA) were used. One displayed the direct current component of the membrane current as a function of applied potential, while the second monitored the quadrature component of the alternating current as obtained via a lock-in amplifier (Ithaco 353; Ithaco, Inc., Ithaca, NY). The slowly changing voltage had a scan rate between 0.03 and 0.1 V s^{-1} unless indicated otherwise; the alternating voltage used was 100 Hz at 2.5 mV amplitude across the cell.

The cells used were made from Teflon. The cell for Mueller-Rudin-type membranes had a total solution volume of ~15 ml; the orifice on which the membrane was formed had a diameter of 2.5 mm. The actual geometric area of the black lipid membrane was measured with a low-power stereo-zoom microscope (American Optical 570; American Optical Scientific Instruments, Warner-Lambert Co., Buffalo, NY) with a micrometer grid in one of its oculars. We estimate that the area measurements so obtained are reliable to within about ±4%. Membranes were made from solutions of *n*-hexane, *n*-decane, *n*-octadecane or squalene (White, 1978), each containing 5 mg lipid per milliliter of solvent. The electrolyte solutions were unbuffered and contained 10, 70, or 500 mM KCl in water or 50 mM KCl in 10 M aqueous $CaCl_2$. This latter solution had been centrifuged to remove debris, and subsequently neutralized with HCl using pH indicator paper. In the experiments with nonactin, its aqueous concentration was 10^{-6} M.

For Takagi-Montal membranes, we used a DuPont type A Teflon film (DuPont Instruments, Wilmimgton, DE), 2.5 μm thick, clamped between two Teflon compartments with a total solution volume of ~8 ml. The film contained a hole of 0.15 to 0.20 mm diameter, which had been punched with a 30 gauge hypodermic syringe needle. The orifice of the hole was coated with one to two μl of a 0.4 (wt/vol)% solution of drugstore-grade Vaseline (petroleum jelly), which had been centrifuged to remove particulates. We estimate the uncertainty in the membrane area to be about ±8%. Membranes were formed by filling the cell compartments with aqueous solution such that the hole was not yet covered, then adding to each solution 10 to 20 μl of hexane containing 10 mg/l of lipid. After ~10 min (to let the hexane evaporate) the levels of the aqueous solutions were raised slowly, one after the other, in order to form the membrane. With the Takagi-Montal method, the cell compartments sometimes contained solutions of different composition, in which case the chloride concentrations in both compartments were equalized by appropriate addition of LiCl to one side.

For both cells, Ag/AgCl electrodes were used; they had surface areas of at least 4 cm^2. No temperature control was used, and the temperature was 22±2°C, with the exception of the measurements using *n*-octadecane as solvent, in which case the temperature was 26±0.5°C.

EXPERIMENTAL RESULTS

Membrane Capacitance

Preliminary capacitance measurements were made, in the absence of nonactin, to verify whether the membrane thickness remained constant, as invariably assumed in the various models. Mueller-Rudin membranes made with hexane as solvent were quite unstable (~60% of them broke during the blackening stage) and short lived (those reaching full blackness typically lasting only 20 to 200 s); they were not considered sufficiently well characterized to record their current-voltage characteristics.

Mueller-Rudin membranes made with *n*-decane were much more stable. While these membranes blackened, their capacitance of course increased with time. However, this increase did not stop after the membranes had become fully black, at a specific capacitance of 0.38 $\mu F\ cm^{-2}$ ±5% at zero applied voltage. Instead, it continued at a much smaller but fairly constant rate of ~2.1 $nF\ cm^{-2}\ min^{-1}$, in accordance with observations reported by Benz and Janko (1976) for dipalmitoyllecithin. The capacitance increase continued until the membrane broke, which occurred at a value of the specific capacitance of 0.41 $\mu F\ cm^{-2}$ at $v = 0$. (The standard deviation of this value is ±4%, and was essentially that of the microscopic determination of the membrane area.) This specific capacitance at membrane breakdown does not depend on the KCl concentration (eight observations each at 10 and 500 mM KCl gave 404 and 412 $nF\ cm^{-2}$, respectively, both with a standard deviation of ±3.4%) but does vary with applied potential. At 200 mV, the specific breakdown capacitance was found to be 0.51 $nF\ cm^{-2}$ (±4%, for 18 membranes) for all KCl concentrations. Thus, the breakdown of our decane-containing black lipid membranes appeared to be deterministic (in terms of membrane capacitance) rather than stochastic (Abidor et al., 1979).

The membrane capacitance has been reported (Babakov et al., 1966; Rosen and Sutton, 1968; White, 1970; Wobschall, 1972; White and Thompson, 1973; Benz and Janko, 1976) to have a voltage dependence of the form

$$C_v = C_{v=0}(1 + \gamma V^2). \tag{18}$$

However, the capacitance of membranes made with decane had a much more complex dependence on voltage than suggested by Eq. 18. Under a voltage scan rate of between 20 and 100 $mV\ s^{-1}$, the capacitance exhibited a very pronounced hysteresis (Schoch et al., 1979). With the voltage starting at zero, the capacitance of newly formed membranes increased approximately according to Eq. 18 until, at about ±125 mV, it started to increase much more rapidly and no longer in an approximately quadratic fashion. On the return sweep after having exceeded ±125 mV, the capacitance remained up to 10% higher until the voltage was approximately zero; the return curve could be described approximately by Eq. 18 with a γ value of the order of 6 V^{-2}. Old membranes exhibited qualitatively similar behavior, although they tended to have a less dramatic change in dC/dV around ±125 mV.

Mueller-Rudin membranes made with *n*-octadecane or squalene formed much more slowly (full blackening could take up to 2 h with sqalene) but, once formed, they had a longer lifetime than those made with decane. Their capacitances were weakly dependent on potential, and could be described by Eq. 18 with γ values ranging from 0.2 to 0.5 V^{-2}. The values of C_{v-0} listed in Table I suggest that relatively little solvent is incorporated and/or that these long, linear solvent molecules are mostly intercalating parallel to the alkyl chains of the lipid molecules, in which case their presence might not much affect the membrane thickness, and hence its capacitance. No capacitance hysteresis was observed with Mueller-Rudin membranes made with either *n*-octadecane or squalene.

The most stable Mueller-Rudin membranes made were those formed in 10 M $CaCl_2$, which is a highly polar aqueous medium containing little if any free water. These membranes will withstand applied voltages of up to 500 mV, which, for steady-state measurements, is rather exceptional. Other than that, the observed capacitance behavior was similar to that of the more dilute KCl solutions: membranes formed with *n*-decane exhibited a strong dependence of capacitance on potential as well as hysteresis, those made with *n*-octadecane or squalene showed only moderate voltage dependencies of C (at most a 5% increase in C between 0 and +0.5 V) and no hysteresis.

Takagi-Montal membranes are more time consuming to make, but have superior stability; they usually survive for more than 24 h and, occasionally, up to 72 h. Their specific capacitance was slightly higher than those of Mueller-Rudin membranes made with squalene, see Table I. (The higher estimated error in the value of C_{v-0} derives from the larger uncertainty in the membrane area.) These membranes exhibited no capacitance hysteresis, and low values of γ, of ~0.1 V^{-2}, resulting in a capacitance change of only ~1% in going from 0 to 300 mV. (Alvarez and Latorre, 1978, reported even lower values, while Benz et al., 1975, observed no voltage dependence of C for Takagi-Montal membranes formed without Vaseline.) The capacitance of our Takagi-Montal membranes decreased in time, by ~5 to 10% in 12 h, after which the capacitance remained fairly constant; we suspect that some hydrocarbon solvent from the Vaseline used to prepare the supporting Teflon film slowly found its way into the lipid membrane. At potentials exceeding +0.3 V, the Takagi-Montal membranes tend to become unstable. If so, they would either break or their capacitance would change suddenly and irreversibly.

TABLE I
SUMMARY OF RESULTS

Membrane type	Solvent used	Specific capacitance	Model and β parameter
		$\mu F\ cm^{-2}$	
Mueller-Rudin	*n*-hexane	0.61 ± 4% (12)	—
Mueller-Rudin	*n*-decane	0.40 ± 4% (20)	*S* 0.36 ± 3% (22)
Mueller-Rudin	*n*-octadecane	0.77 ± 5% (8)	*C* 0.26 ± 4% (7)
Mueller-Rudin	squalene	0.85 ± 4% (14)	*C* 0.25 ± 5% (5)
Takagi-Montal	—	0.95 ± 10% (15)	*C* 0.30 ± 3% (18)

The specific capacitance was measured in 10, 70, and 500 mM aqueous KCl in the absence of nonactin. The model parameter β for ion transport for either the single jump model, *S*, or the continuum model, *C*, was determined in the same aqueous solutions in the presence of 1 μM nonactin. The β values obtained in 10 M $CaCl_2$ were significantly lower. The standard deviations, in percentage, are followed by the number of membranes tested, in parentheses.

Steady-State Current-Voltage Curves

Currents were measured as a function of applied voltage at 10-mV intervals. In Fig. 3 we show some examples of curves of $\log[(c_{w0}e^{v/2} - c_{w1}\ e^{-v/2})/i]$ vs. potential for membranes that showed no capacitance hysteresis. Comparison of the shapes of the curves in Fig. 3 with those of Fig. 2 clearly indicates that the single jump description does not apply to these data. To test whether the continuum model can accomodate these observations quantitatively, we have compared the measured currents with those calculated from $i/B = (c_{w0} - c_{w1}\ e^{-v})/(e^{-\beta v} - e^{\beta - 1v})$, where B and β are adjustable parameters. Adjustment of the two parameters, B and β, is quite easy since they hardly interact, B being a scale factor for the current and β for the voltage. Fig. 4 shows that such a residual analysis, performed on a PDP 11-23 minicomputer (Digital Equipment Corp., Marlboro, MA), is quite sensitive to small variations in β.

All current-voltage curves obtained with Mueller-Rudin membranes made with *n*-octadecane or squalene, in aqueous KCl as well as in $CaCl_2$ solutions, could be fitted quantitatively, i.e., to within ±3%, to the voltage dependence of Eq. 10 over the entire range of potentials used. The same applied to Takagi-Montal membranes, up to the potential at which their capacitance changed suddenly. At that point the current would exhibit sudden noise spikes, possibly from field-induced membrane imperfections (Wei and Woo, 1973; Coster and Zimmermann, 1975*a*, *b*; Benz et al., 1979).

As long as the voltage excursions did not exceed ±125 mV, the current-voltage curves obtained with Mueller-Rudin membranes made with *n*-decane could be fitted with either model. The fit seemed somewhat better with the continuum model, but the voltage range was too limited to make a definite choice. With larger voltage excursions, the data could no longer be fitted to Eq. 10 but could still be represented quantitatively by the single jump relation (Eq. 14). The current-voltage curves exhibited a hysteresis paralleling that of the capacitance, see Fig. 5, and fitting the forward and reverse traces required different values of

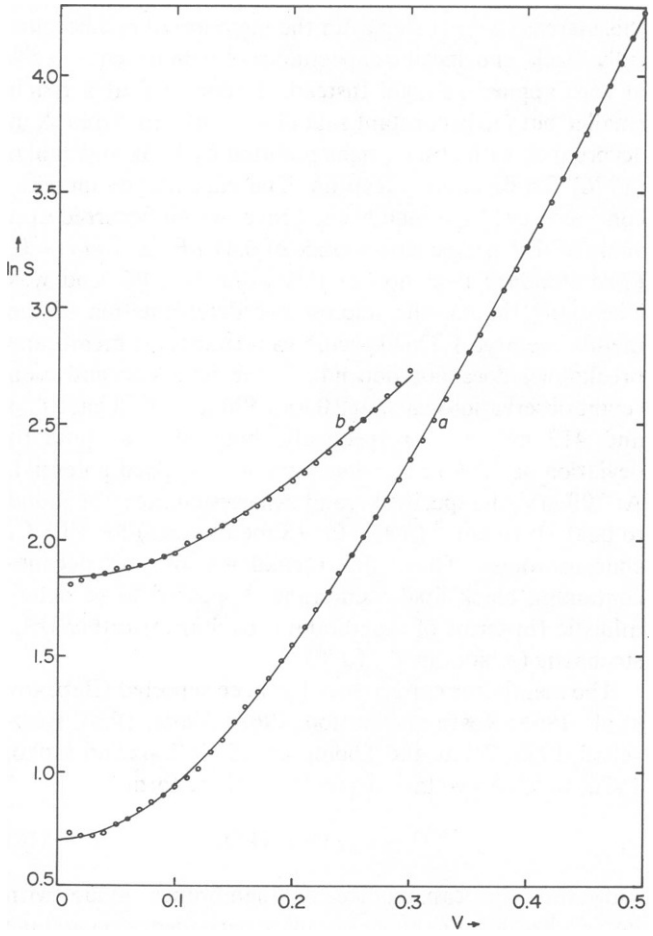

FIGURE 3 Two experimental data sets, plotted as ln *S* vs. *V*, where *S* has the dimension of M/nA and *V* is in volts. (*a*) Mueller-Rudin membrane made from diphytanoyllecithin in octadecane, in aqueous 10 M $CaCl_2$ + 50 mM KCl + 1 μM nonactin. (*b*) Takagi-Montal membrane made from diphytanoyllecithin in aqueous 70 mM KCl + 1 μM nonactin. Points, experimental data; lines drawn according to Eq. 10 using (*a*) β = 0.193 and (*b*) β = 0.29.

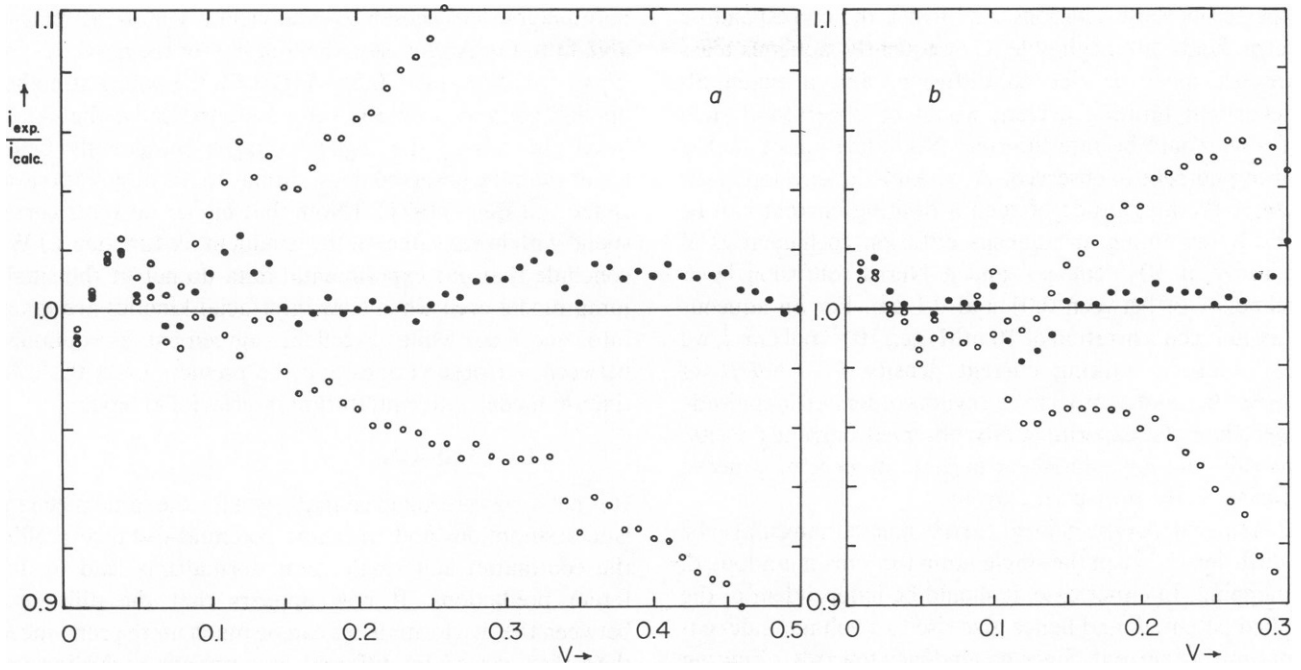

FIGURE 4 The sensitivity to β of the fit of the experimental data of Fig. 3 to Eq. 10. Plotted is the ratio of the experimental current to that calculated from Eq. 10, for (*a*) the solution of Fig. 3 *a* and $\beta = 0.18$ (*top* open circles), $\beta = 0.193$ (filled circles) and $\beta = 0.20$ (*bottom* open circles; (*b*) the solution of Fig. 3 *b* and $\beta = 0.28$ (*top* open circles), $\beta = 0.29$ (filled circles) and $\beta = 0.30$ (*bottom* open circles). Note that the full vertical scale encompasses only ±10%.

β. Under these conditions, the membrane thickness is clearly no longer constant. Since both the continuum and the single jump results used here require that the membrane thickness be constant, we do not consider the results with decane-containing Mueller-Rudin membranes relevant to our search for the appropriate model description of ion transport.

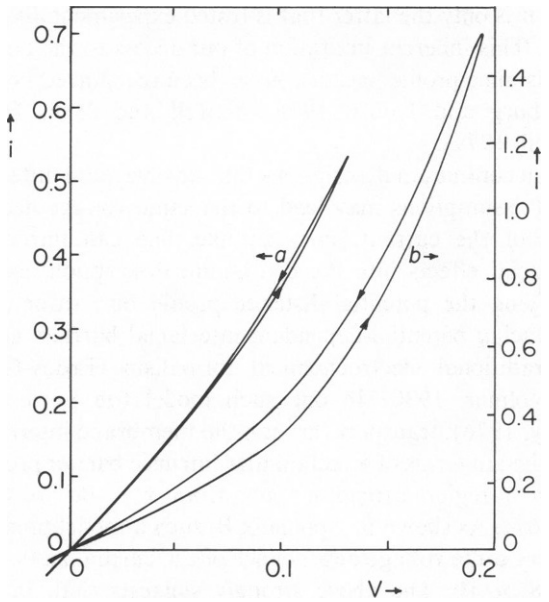

FIGURE 5 Current-voltage curves obtained with Mueller-Rudin membranes made from diphytanoyllecithin in decane, recorded with a voltage scan rate of 100 mV s^{-1}. Aqueous solutions: 0.5 M KCl + 1 μ nonactin. Currents in microamperes, potential in volts. As long as the voltage excursion does not exceed ±125 mV, the current-voltage curves exhibit only minor hysteresis; for larger voltage excursions, the hysteresis increases markedly.

Validity of the Mechanistic Assumptions Made

The nonactin-mediated transport of potassium ions is a complex process involving several individual steps. Consequently, the simplifying mechanistic assumptions used to derive Eqs. 10 and 14 need justification. The processes involved can be enumerated as follows.

1. In order for potassium ions to permeate the membrane, they must first reach the membrane-water interface. Moreover, after passing through the membrane, they must be removed from the other membrane-water interface. Such aqueous mass transport could limit or influence the measured current.

2. In the steady state, the membrane must support a net flux of nonactin molecules equal in magnitude to that of potassium-nonactin complexes, but flowing in the opposite direction. Thus, carrier transport across the membrane could limit or influence the current.

3. Before a potassium ion can cross the membrane, it must first form a complex with its carrier, nonactin. Likewise, this complex must dissociate when the potassium ion is released at the other side of the membrane. Therefore, the rates of formation and of dissociation of the cation-carrier complex could limit or influence the current. Below we will consider these potential complications one by one.

1. The products of the measured current and the resistance of the aqueous solutions indicate that the voltage

drops across these solutions, and hence the corresponding electric fields, are negligible. Consequently, aqueous mass transport must be due to diffusion, and a potential-independent limiting current would be observed if such diffusion would be rate limiting. No indication of such a limiting current is observed. A back-of-the-envelope estimate of the magnitude of such a limiting current can be made by assuming an aqueous diffusion coefficient D of the order of 10^{-5} cm^2 s^{-1} and a Nernst diffusion layer thickness δ of between 0.01 and 0.1 cm. For an aqueous potassium concentration of 10 mM, i.e., 10^{-5} mol cm^{-3}, we then obtain a limiting current density $I = FcD/\delta$ of between 0.1 and 1 mA cm^{-2}, several orders of magnitude larger than the experimentally observed current density. This rules out any significant partial influence of aqueous diffusion on the measured current.

2. Transport of the neutral carrier nonactin must also be by diffusion or, when the single jump formalism is adopted, by hopping. In either case, it should be independent of the applied potential, and hence give rise to a voltage-independent limiting current. Since no tendency towards a limiting current is observed, even at the highest potentials, we can rule out any major involvement of carrier transport. Even a minor measurable effect of carrier diffusion is ruled out by the fact that, at constant nonactin concentration, the shapes of the current-voltage curves for 10, 70, and 500 mM KCl are identical.

3. The assumption that the complexation and dissociation reactions are sufficiently fast can be justified in a similar fashion. The rates of interfacial chemical reactions can be expected to be independent of applied potential (or, at most, to be weakly potential-dependent, as in the model used in Appendix B). The observed current-voltage curves show no tendency to level off and, to quote Läuger and Stark (1970), "From the absence of a limiting current we may therefore conclude that the slowest step in the ion transport is the migration of the complex across the interior of the membrane."

The above argument does not eliminate the possibility of a relatively minor influence on the current, especially at the larger applied voltages. Since our analysis deals with (and draws conclusions from) rather small differences, the point cannot be brushed aside, and has been considered in somewhat more detail.

In Appendix A we derive current-voltage relations for the continuum and single jump models that include slow interfacial kinetics. We have attempted to fit our experimental data to Eqs. A3 and A6. As expected, agreement between our data and Eq. A3 was best when the interfacial rate constants were approaching infinity (while keeping constant their ratio $k_C/k_D = K_N$). Satisfactory agreement between our data and Eq. A6 could not be achieved, and it will be clear from Fig. 6 in Appendix A why this was so: despite the use of an additional adjustable parameter, k°/k_D, the predicted curves exhibit only a superficial resemblance to the experimental ones. Whenever the rate parameters were chosen so as to yield a somewhat reasonable fit to Eq. A6 for, say, the first half of the curve (as for $k^\circ/k_D = 0.02$ and $\beta = 0.5$ in Fig. 6 *f*), the points at higher applied voltages would deviate systematically, the calculated currents at the higher voltages consistently being lower than the observed ones, similar to the observations of Stark and Benz (1971). (Note that higher currents correspond with lower values of the conductance function s.) We conclude that our experimental data do not fit the single jump model even when slow interfacial kinetics are taken into account, while excellent agreement is obtained between our observations and the predictions of the continuum model with equilibrium interfacial kinetics.

DISCUSSION

It is not always recognized that, even for the same mechanistic assumptions and the same potential-distance profile, the continuum and single jump formalisms lead to different predictions. It now appears that the difference between the two formalisms can be much more pronounced than that caused by different assumptions regarding the potential profile. For example, when the trapezoidal profile $\psi(x)$ is replaced by a continuous analytical function, as was done by Hall et al., (1973) and by de Levie (1978), the predicted results are essentially indistinguishable as long as the continuum formalism is used. This is a consequence of the fact that many assumed profiles $\psi(x)$ can lead to the same value of the integral

$$\int_0^d e^{\psi} dx$$

while it is only the latter that is tested experimentally, see Eq. 4. This inherent limitation of our access to the potential-distance profile has, of course, been recognized before (Ginsburg and Noble, 1976; Attwell and Jack, 1978; Attwell, 1979).

Even continuum descriptions that involve quite different model assumptions may lead to the same voltage dependence of the current. For example, one can introduce interfacial effects into the continuum description not by modifying the potential-distance profile but, rather, by introducing potential-dependent interfacial barriers using the traditional electrochemical formalism (Erdey-Grúz and Volmer, 1930) In one such model (de Levie and Abbey, 1976), transport through the membrane interior is described in terms of a rectangular intrinsic barrier profile, but in a region extending only from $x = \beta d$ to $x - (1 - \beta)d$. As shown in Appendix B, such a model predicts the very same voltage dependence of the current as that of Eqs. 8 or 10. The above strongly suggests that, in the present study, we are not so much testing a particular profile as we are probing the correctness of the underlying models, continuum vs. single jump.

It might be argued that, even when various continuum models predict similar voltage dependencies of the current, this need not be the case for the single jump model. This,

however, appears to be rather unlikely, unless the single jump formalism were restructured completely to make the position of the barrier maximum a function of applied potential. The original single barrier calculations put the barrier maximum in the middle of the membrane. The trapezoidal profile used here moves that maximum to an arbitrary position, dependent on the sign but not on the magnitude of the applied potential. The assumption that the position of the maximum does not vary with applied potential is, of course, consistent with the basic tenet that the barrier is so high that the position of its maximum is not materially affected by v.

In summary, then, and disregarding those cases in which the measured capacitance exhibits a very pronounced voltage dependence and hysteresis, the shapes of the steady-state current voltage curves reported here can be represented quantitatively by the continuum approach, but not by the corresponding single jump model. Our data also indicate that, for nonactin-mediated potassium transport, the rates of the interfacial reactions are much higher than those of ion permeation through the membrane.

APPENDIX A

The Effect of Slow Interfacial Kinetics

We now extend the continuum treatment to include interfacial kinetics by equating the net ionic flux I/F across the membrane to the net interfacial kinetic flux. Results are given here for carrier-mediated transport; those for lipophilic ions are obtained simply by substituting k_W for $k_C c_N$ or $k_C n_N$, k_M for k_D and $K = k_W/k_M$ for $K_N = k_C/k_D$. We have

$$\frac{I}{F} = -D_M\left(\frac{dc_M}{dx} + c_M\frac{d\psi}{dx}\right) = k_C c_{W0} c_N - k_D c_{M0} = k_D c_{M1} - k_C c_{W1} c_N \quad \text{(A1)}$$

or, after substitution of Eqs. 4 and 6

$$\frac{D_M v\,(c_{M0} - c_{M1}e^{-v})}{[e^{-\beta v} - e^{(\beta-1)v}]e^{\psi_0} d} = k_C c_{W0} c_N - k_D c_{M0} = k_D c_{M1} - k_C c_{W1} c_N. \quad \text{(A2)}$$

Eq. A2 allows us to solve for c_{M0} and c_{M1}, whereupon we obtain

$$I = \frac{FD_M v\,(c_{M0} - c_{M1}e^{-v})}{[e^{-\beta v} - e^{(\beta-1)v}]e^{\psi_0} d} = \frac{FD_M v k_C c_N (c_{W0} - c_{W1}e^{-v})}{D_M v\,(1 + e^{-v}) + e^{\psi_0} k_D d\,(e^{-\beta v} - e^{[\beta-1]v})} \quad \text{(A3)}$$

$$S = \frac{c_{W0} - c_{W1}e^{-v}}{Ie^{-v/2}} = \frac{e^{\psi_0} d[e^{(1/2-\beta)v} - e^{-(1/2-\beta)v}]}{FD_M K_N c_N v} + \frac{e^{v/2} + e^{-v/2}}{Fk_C c_N}. \quad \text{(A4)}$$

The first term on the right-hand side of Eq. A4 is the same as one would derive from Eq. 10, while the second term reflects the effect of nonequilibrium interfacial kinetics.

For the single jump model, Eqs. 11 and 12 yield likewise

$$\frac{I}{F} = \vec{k} n_{M0} - \overleftarrow{k} n_{M1} = k^o n_{M0} e^{\beta v} - k^o n_{M1} e^{(\beta-1)v} = k_C c_{W0} n_N - k_D n_{M0} = k_D n_{M1} - k_C c_{W1} n_N, \quad \text{(A5)}$$

from which n_{M0} and n_{M1} can be found. Hence

$$I = Fk^o[n_{M0}e^{\beta v} - n_{M1}e^{(\beta-1)v}] = \frac{Fk_C n_N k^o e^{\beta v}(c_{W0} - c_{W1}e^{-v})}{k_D + k^o e^{\beta v}(1 + e^{-v})} \quad \text{(A6)}$$

$$S = \frac{c_{W0} - c_{W1}e^{-v}}{Ie^{-v/2}} = \frac{e^{(1/2-\beta)v}}{FK_N n_N k^o} + \frac{e^{v/2} + e^{-v/2}}{Fk_C n_N}. \quad \text{(A7)}$$

The additional term in Eq. A7 due to the slow interfacial kinetics is fully equivalent to that in Eq. A4, since the two models treat the interfacial kinetics in a similar way. The dimensionless conductance function s follows from Eq. A7 as

$$s = \frac{S_v}{S_{v=0}} = \frac{e^{(1/2-\beta)v} + (e^{v/2} + e^{-v/2})k^o/k_D}{1 + 2k^o/k_D}. \quad \text{(A8)}$$

Fig. 6 illustrates some curves of s vs. v predicted by Eq. A8 for various values of β and k^o/k_D. For ease of comparison, Fig. 6 also contains the curves and data shown in Fig. 3. When nonequilibrium interfacial kinetics are taken into account in the single jump model, the simple criterion suggested by Fig. 2 no longer applies. However, Fig. 6 also shows quite unambiguously the inability of Eq. A8 to represent the experimental data.

APPENDIX B

An Alternative Continuum Model

In the preceding discussion of the continuum model, the interfacial aspects of the membrane were incorporated in the formalism through an assumed trapezoidal potential-distance profile, its sloping sides representing the combined effects of image forces and dipole potentials acting on the ions in the membrane. At the metal-solution interface, the analogous problem is traditionally handled by introducing interfacial potential-energy barriers. This approach goes back to the work of Erdey-Grúz and Volmer (1930) and has since been applied by several authors to ion transport through membranes (Zwolinsky et al., 1949; Wei and Woo, 1974; Hladky, 1974; de Levie and Abbey, 1976; Ciani, 1976).

Fig. 7 illustrates the model used here (de Levie and Abbey, 1976). The interfacial barriers are characterized by transfer coefficients, which, in Fig. 7, have been given a geometric representation. As in the single jump model, the detailed shape of the interfacial barriers is not considered. The continuum approach is applied only to transport through the central portion of the model, for $\beta < x/d < (1 - \beta)$. For c_M and c_N (but not for c_W) the index 0 now refers to $x/d = \beta$ and, similarly, 1 refers to $x/d = 1 - \beta$. For a lipophilic ion we then derive from Eq. 3,

$$\frac{I}{FD_M}\int_{\beta d}^{(1-\beta)d} e^{\psi} dx = c_{M0}e^{\psi_0 - \beta v} - c_{M1}e^{\psi_0 + (\beta-1)v}. \quad \text{(B1)}$$

The integral on the left-hand side of Eq. B1 has, exactly, the value given in Eq. 6, while interfacial partition equilibrium now yields

$$c_{M0} = Ke^{-\psi_0 + \beta v} c_{W0}, \qquad c_{M1} = Ke^{-\psi_0 - \beta v} c_{W1} \quad \text{(B2)}$$

so that the current density is given by

$$I = \frac{FD_M K v(c_{W0} - c_{W1}e^{-v})}{e^{\psi_0} d[e^{-\beta v} - e^{(\beta-1)v}]}, \quad \text{(B3)}$$

which is identical to Eq. 8. For cation transport mediated by a neutral carrier, under the assumed conditions,

$$c_{M0} = K_N c_N e^{-\psi_0 + \beta v} c_{W0}, \qquad c_{M1} = K_N c_N e^{-\psi_0 - \beta v} c_{W1} \quad \text{(B4)}$$

so that

$$I = \frac{FD_M K_N c_N v (c_{W0} - c_{W1} e^{-v})}{e^{\psi_0} d[e^{-\beta v} - e^{(\beta - 1)v}]}, \quad \text{(B5)}$$

which is indistinguishable from Eq. 10. Only when nonequilibrium interfacial kinetics need be considered do these two continuum models predict different current-voltage curves; in the present case, no such need exists.

C. van Dijk was the recipient of a North Atlantic Treaty Organization Science Fellowship supplied by the Netherlands Organization for the Adavncement of Pure Research (ZWO). R. de Levie gratefully acknowledges financial support from the National Institutes of Health grant 5RO1 12256-18.

Received for publication 26 November 1984.

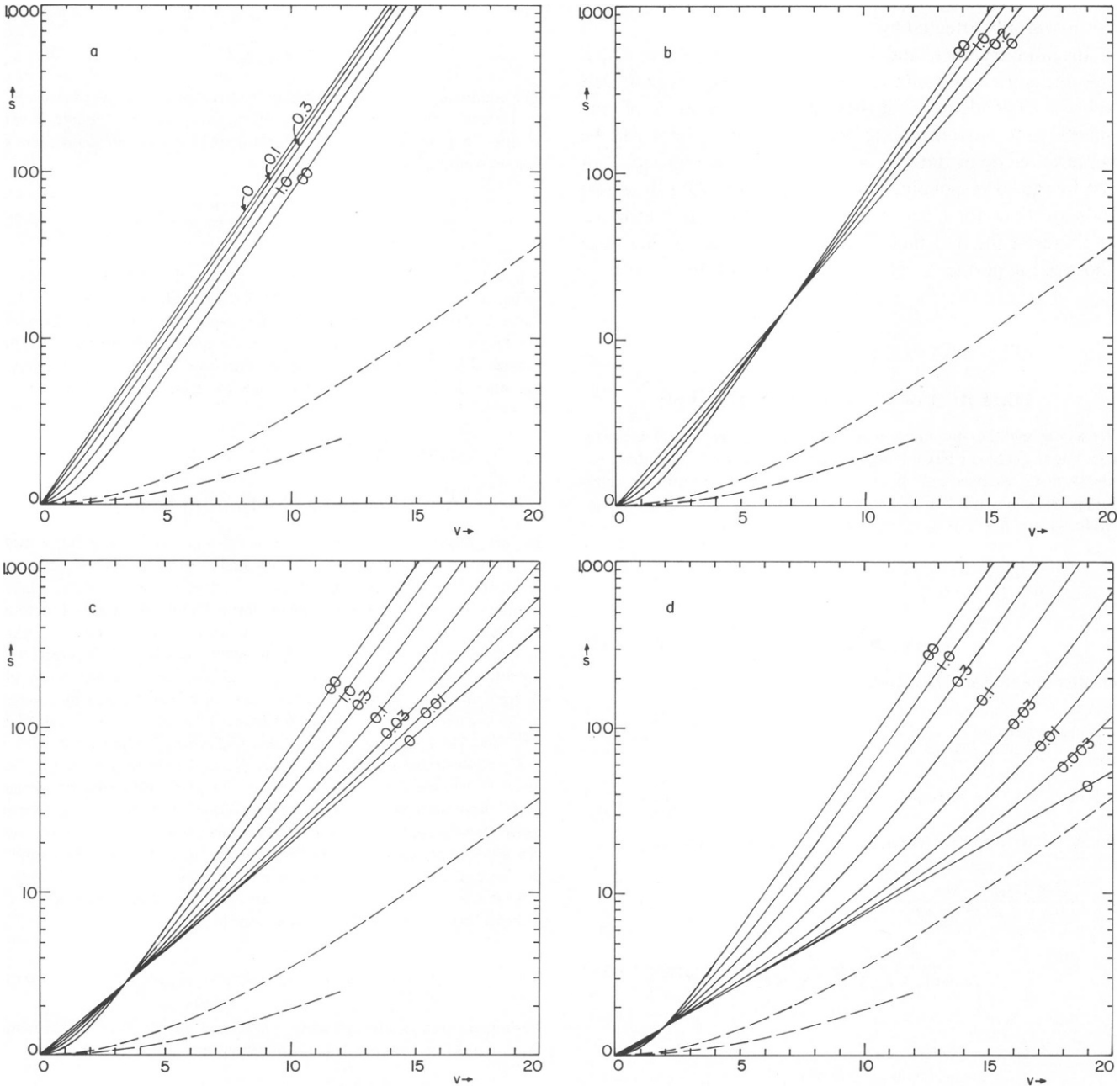

FIGURE 6 Semilogarithmic representation of the dimensionless conductance function s of Eq. A8 for the single jump model with nonequilibrium interfacial kinetics for various values of β and k^o/k_D. Values of β are (*a*) $\beta = 0{,}0$; (*b*) $\beta = 0.1$; (*c*) $\beta = 0.2$; (*d*) $\beta = 0.3$; (*e*) $= 0.4$, and (*f*) $\beta = 0.5$. Values of k^o/k_D are given with the curves. Also shown, as broken lines, are two curves according to Eq. 10 for $\beta = 0.193$ and $\beta = 0.29$, respectively, representing the experimental data of Fig. 3.

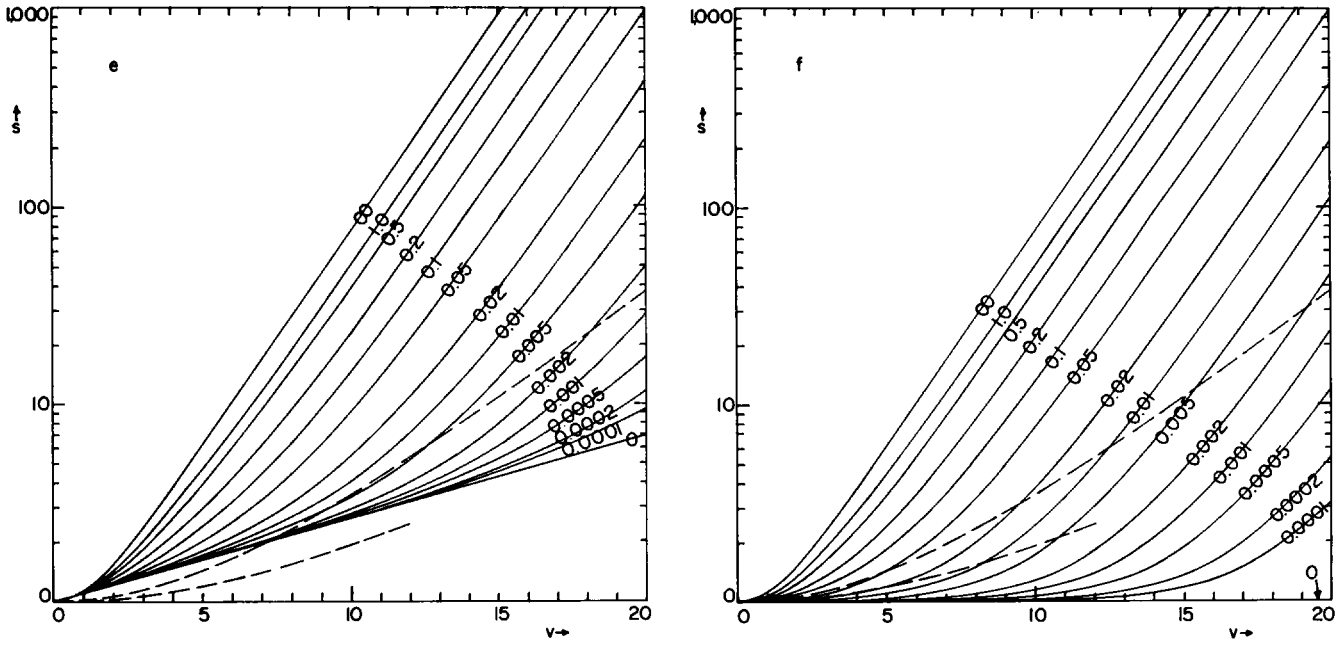

FIGURE 6 Continued

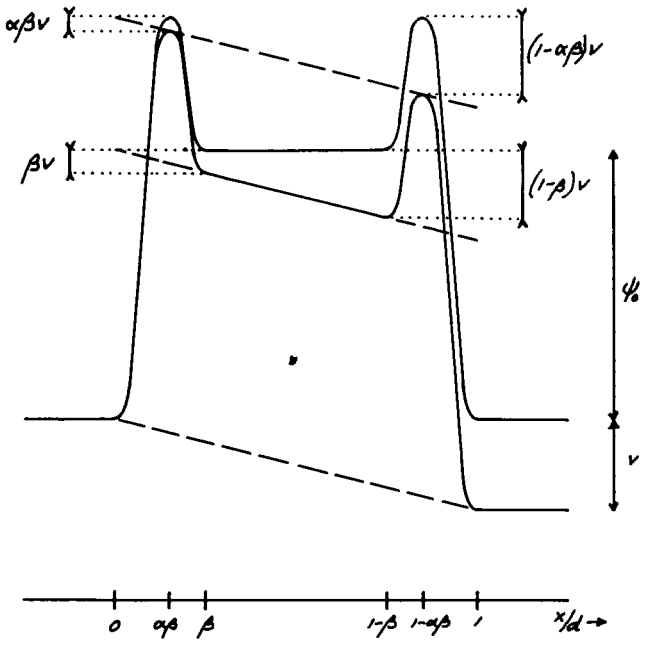

FIGURE 7 The potential-distance profile used by de Levie and Abbey (1976), with interfacial barriers for $0 \leq x/d \leq \beta$ and $(1 - \beta) \leq x/d \leq 1$, and continuum treatment for the membrane interior at $\beta \leq x/d \leq (1 - \beta)$. *Top* and *bottom* curves are without and with an externally applied voltage v, respectively. Potentials are expressed in units of kT/e; α is a transfer coefficient.

REFERENCES

Abidor, I. G., V. B. Arakelyan, L. V. Chernomordik, Yu. A. Chizmadzhev, V. F. Pastushenko, and M. R. Tarasevich. 1979. Electric breakdown of bilayer lipid membranes. I. The main experimental facts and their qualitative discussion. *Bioelectrochem. Bioengin.* 6:37–52.

Alvarez, O., and R. Latorre. 1978. Voltage-dependent capacitance in lipid bilayers made from monolayers. *Biophys. J.* 21:1–17.

Andrews, D. M., E. D. Manev, and D. A. Haydon. 1971. Composition and energy relationships for some thin lipid films, and the chain conformation in monolayers at liquid-liquid interfaces. *Spec. Disc. Faraday Soc.* 1:46–56.

Attwell, D., and J. Jack. 1978. The interpretation of membrane current-voltage relations: a Nernst-Planck analysis. *Prog. Biophys. Mol. Biol.* 34:81–107.

Attwell, D. 1979. Problems in the interpretation of membrane current-voltage relations. *Membr. Transp. Processes.* 3:298–41.

Babakov, A. V., L. N. Ermishkin, and E. A. Liberman. 1966. Influence of electric field on the capacity of phospholipid membranes. *Nature (Lond.).* 210:953–955.

Benz, R., O. Fröhlich, P. Läuger, and M. Montal. 1975. Electrical capacity of black lipid films and of lipid bilayers made from monolayers. *Biochim. Biophys. Acta.* 394:323–334.

Benz, R., and K. Janko. 1976. Voltage-induced capacitance relaxation of lipid bilayer membranes. Effects of membrane composition. *Biochim. Biophys. Acta.* 455:721–738.

Benz, R., F. Beckers, and U. Zimmermann. 1979. Reversible electrical breakdown of lipid bilayer membranes: a charge-pulse relaxation study. *J. Membr. Biol.* 48:181–204.

Born, M. 1920. Volumen und Hydratationswarme der Ionen. *Z. Physik.* 1:45–48.

Bunce, A.S., and R.C. Hider. 1974. The composition of black lipid membranes formed from egg-yolk lecithin, cholesterol and *n*-decane. *Biochim. Biophys. Acta.* 363:423–427.

Ciani, S. 1976. Influence of molecular variations of ionophore and lipid on the selective ion permeability of membranes. II. A theoretical model. *J. Membr. Biol.* 30:45–63.

Coster, H. G. L., and U. Zimmermann. 1975*a*. Direct demonstration of dielectric breakdown in the membranes of *Valonia utricularis*. *Z. Naturforsch. Teil C Biosci.* 30:77–79.

Coster, H. G. L., and U. Zimmermann. 1975*b*. Dielectric breakdown in the membranes of *Valonia utricularis*. The role of energy dissipation. *Biochim. Biophys. Acta.* 382:410–418.

Erdey-Grúz, T., and M. Volmer. 1930. Zur Theorie der Wasserstoffüberspannung. *Z. Phys. Chem. Abt. A.* 150:203–213.

Fettiplace, R., D. M. Andrews, and D. A. Haydon. 1971. The thickness, composition and structure of some lipid bilayers and natural membranes. *J. Membr. Biol.* 5:277–296.

Finkelstein, A., and A. Cass. 1968. Permeability and electrical properties of thin lipid membranes. *J. Gen. Physiol.* 52(Suppl.):145S–172S.

Ginsburg, S., and D. Noble. 1976. Use of current-voltage diagrams in locating peak energy barriers in cell membranes. *J. Membr. Biol.* 29:211–229.

Goldman, D. E. 1943. Potential, impedance, and rectification in membranes. *J. Gen. Physiol.* 27:37–60.

Hall, J. E., C. A. Mead, and G. Szabo. 1973. A barrier model for current flow in lipid bilayer membranes. *J. Membr. Biol.* 11:75–97.

Hladky, S. B. 1974. The energy barriers to ion transport by nonactin across thin lipid membranes. *Biochim. Biophys. Acta.* 352:71–85.

Ketterer, B., B. Neumcke, and P. Läuger. 1971. Transport mechanism of hydrophobic ions through lipid bilayer membranes. *J. Membr. Biol.* 5:225–245.

Läuger, P., and G. Stark. 1970. Kinetics of carrier-mediated ion transport across lipid bilayer membranes. *Biochim. Biophys. Acta.* 211:458–466.

de Levie, R., and H. Moreira. 1972. Transport of ions of one kind through thin membranes. I. General and equilibrium considerations. *J. Membr. Biol.* 9:241–260.

de Levie, R., N. G. Seidah, and H. Moreira. 1972. Transport of ions of one kind through thin membranes. II. Nonequilibrium steady-state behavior. *J. Membr. Biol.* 10:171–192.

de Levie, R., and K. M. Abbey. 1976. A unified approach to ion transport through membranes. I. Membrane-soluble ions. *J. Theor. Biol.* 56:151–73.

de Levie, R. 1978. Mathematical modeling of transport of lipid- soluble ions and ion-carrier complexes through lipid bilayer membranes. *Adv. Chem. Phys.* 37:99–137.

MacGillivray, A. D., and D. Hare. 1969. Applicability of Goldman's constant field assumption to biological systems. *J. Theor. Biol.* 25:113–126.

Markin, V. S. 1969. The impedance of artificial bimolecular phospholipid membranes in the presence of ion carriers. *Mol. Biol. (Engl. Trans. Mol. Biol. [Mosc.]).* 3:610–616.

Montal, M., and P. Mueller. 1972. Formation of bimolecular membranes from lipid monolayers and a study of their electrical properties. *Proc. Natl. Acad. Sci. USA.* 69:3561–3566.

Montal, M. 1974. Formation of bimolecular membranes from lipid monolayers. *Methods Enzymol.* 32:545–554.

Mott, N. F. 1937. The theory of crystal rectifiers. *Proc. R. Soc. Lond. A Math. Phys. Sci.* 171:27–38.

Mueller, P., D. O. Rudin, H. T. Tien, and W. C. Wescott. 1962*a*. Reconstitution of cell membrane structure in vitro and its transformation into an excitable system. *Nature (Lond.).* 194:979–980.

Mueller, P., D. O. Rudin, H. T. Tien, and W. C. Wescott. 1962*b*. Reconstitution of excitable cell membrane structure in vitro. *Circulation.* 26:1167–1170.

Mueller, P., D. O. Rudin, H. T. Tien, and W. C. Wescott. 1963. Methods for the formation of single bimolecular lipid membranes in aqueous solution. *J. Phys. Chem.* 67:534–535.

Nernst, W. 1888. Zur Kinetik der in Lösung befindlichen Körper. *Z. Phys. Chem.* 2:613–637.

Nernst, W. 1889. Die elektromotorische Wirksamkeit der Ionen. *Z. Phys. Chem.* 4:129–181.

Neumcke, B., and P. Läuger. 1969. Nonlinear electrical effects in lipid bilayer membranes. II. Integration of the general Nernst-Planck equations. *Biophys. J.* 9:1160–1170.

Pagano, R. E., J. M. Ruysschaert, and I. R. Miller. 1972. The molecular composition of some lipid bilayer membranes in aqueous solution. *J. Membr. Biol.* 10:11–30.

Parsegian, A. 1969. Energy of an ion crossing a low dielectric membrane: solutions to four relevant electrostatic problems. *Nature (Lond.).* 221:844–846.

Planck, M. 1890. Über die Erregung von Electricität und Wärme in Electrolyten. *Ann. Phys. Chem. Neue Folge.* 39:161–186.

Rosen, D., and A. M. Sutton. 1968. The effects of a direct current potential bias on the electrical properties of bimolecular lipid membranes. *Biochim. Biophys. Acta.* 163:226–233.

Schoch, P., D. F. Sargent, and R. Schwyzer. 1979. Capacitance and conductance as tools for the measurement of asymmetric surface potentials and energy barriers of lipid bilayer membranes. *J. Membr. Biol.* 46:71–89.

Stark, G., and R. Benz. 1971. The transport of potassium through lipid bilayer membranes by the neutral carriers valinomycin and monactin. *J. Membr. Biol.* 5:133–153.

Stark, G. 1973. Rectification phenomena in carrier-mediated ion transport. *Biochim. Biophys. Acta.* 298:323–332.

Takagi, M., K. Azuma, and U. Kishimoto. 1965. A new method for the formation of bilayer membranes in aqueous solution. *Annu. Rep. Biol. Works Fac. Sci. Osaka Univ.* 13:107–110.

Wei, L. Y., and B. Y. Woo. 1973. Ion transport through thin lipid films. *J. Biol. Phys.* 1:50–68.

Wei, L. Y., and B. Y. Woo. 1974. Semiconductor theory of ion transport in thin lipid membranes. I. Potential and field distributions. *Bull. Math. Biol.* 36:229–245.

White, S. H. 1970. A study of lipid bilayer membrane stability using precise measurements of specific capacitance. *Biophys. J.* 10:1127–1148.

White, S. H., and T. E. Thompson. 1973. Capacitance, area, and thickness variations in thin lipid films. *Biochim. Biophys. Acta.* 323:7–22.

White, S. H. 1978. Formation of "solvent-free" black lipid bilayer membranes from glyceryl monooleate dispersed in squalene. *Biophys. J.* 23:337–347.

Wobschall, D. 1972. Voltage dependence of bilayer membrane capacitance. *J. Colloid Interface Sci.* 40:417–423.

Zwolinski, B. J., H. Eyring, and C. E. Reese. 1949. Diffusion and membrane permeability. *J. Phys. Colloid Chem.* 53:1426–1453.